Human-Driven Trophic Changes in a Large, Shallow Urban Lake: Changes in Utah Lake, Utah from Pre-European Settlement to the Present

Richard Williams · Stephen Nelson ⬤ · Samuel Rushforth · Kevin Rey · Gregory Carling · Barry Bickmore · Adam Heathcote · Theron Miller · Leland Meyers

Abstract Lakes are invaluable archives of past ecosystem changes, and this study focuses on one of the largest freshwater lakes in the western US. At 380 km^2, Utah Lake is the third-largest freshwater lake in the USA west of the Mississippi River. Adjacent to an urban corridor, it is an important resource for surrounding communities as well as being impacted by them. Recently, large harmful algal blooms have drawn attention to its ecosystem health, and a rapidly growing population and recent lengthy drought continue to stress the lake. Its sedimentary record is an important archive of human impacts to ecosystems. Three freeze cores were obtained in 2019 to investigate environmental changes and human impacts since European settlement began in ~1850. After establishing core chronologies using ^{210}Pb, ^{137}Cs and correlation, proxies investigated included pollen, C- and N-isotopes, nutrients (C, N, and P), and heavy metal abundances. Low C:N ratios indicated that organic matter budget was dominated algae rather than plant debris. Discernable increases in nutrients began in the mid-twentieth century, whereas increases in Pb began as early as ~1900. Nutrient increases were related to agricultural runoff and variably treated sewage effluent, whereas heavy metal loading was due to heavy industry (iron and steel), coal combustion, and urban runoff. Over the last several decades, nutrient and metal loadings have stabilized, indicating a steady state has been reached. Gains in nutrient removal from effluent have been offset by growing populations and decreases in heavy industry and coal combustion have been countered by urbanization. Overall, the lake has been continually oxic, with possible episodes of anoxia during algal blooms. This study also provides a measure of pre_Eurpopean ecosystem health using geochemical baselines in order to establish reasonable water-quality standards.

Keywords Utah Lake · Eutrophication · Algal blooms · Modern sediments · Pyrolysis · Stable isotopes

R. Williams · S. Nelson (✉) · K. Rey · G. Carling · B. Bickmore
Department of Geological Sciences, S-389 ESC, Provo, UT 84602, USA
e-mail: oxygen.isotope@gmail.com

S. Rushforth
Rushforth Phycology, 452 N Palisades Dr. Orem, Orem, UT 84057, USA

A. Heathcote
St. Croix Watershed Research Station, Science Museum of Minnesota, 16910 152nd St. N., Marine on St Croix, MN 55047, USA

T. Miller · L. Meyers
Wasatch Front Water Quality Council, 1800 West 1200 North, West Bountiful, UT 84047, USA

1 Introduction

A rise in the frequency of harmful algal blooms (HABs) in lakes around the world has spurred an interest in the role anthropogenic influences play in the eutrophication of shallow lakes (Burford et al., 2020). As a measure of this interest, a recent search on the Web of Science returned nearly 900 publications on the topic with both "eutrophication" and "lake" in the title, as well as more than 800 publications with the phrase "harmful algal bloom" (WS, 2021). A current focus is on human settlement around shallow lakes and how this drives eutrophication and affects nutrient levels leading to HABs (Smith & Schindler, 2009), which are detrimental to fish and wildlife, as well as humans (Chislock et al., 2013; Landsberg, 2002; Zanchett & Oliveria-Filho, 2013). As increased organic matter near the sediment-water interface is consumed by bacteria, harmfully low dissolved oxygen levels may be realized (Zhu et al., 2008).

We refer to the combined contributions of urban and agricultural impacts to elevated nutrients in the lake as anthropogenically influenced discharge, or AID. As discussed below, the current sources of AID are fairly well documented and prior studies have estimated the balance between natural and human sources. The purpose of this study is to understand the influence that population growth has had on the nutrient and metal loading of shallow lakes, specifically in Utah Lake, since European settlement and urbanization (Fig. 1). The value in establishing pre-European conditions is that remedial actions cannot improve ecosystem health any further, thereby assisting in the establishment of long-term goals to limit AID. Realistic water-quality goals can be set somewhere between current and pre-settlement conditions.

Utah Lake (Fig. 1) lies along an urban corridor that has undergone exponential population growth since European settlement began in ~1850 (Fig. 2) and has received changing fluxes of variably treated wastewater, industrial discharges, storm, and agricultural runoff. As such, it is an ideal location for a retrospective study of the human impacts on lake ecology through the study of its sedimentary archive through mineralogical, geochemical, isotopic, and microfossil proxies, once core chronologies are established by ^{210}Pb and ^{137}Cs methods.

1.1 Limnological Setting

Utah Lake is located in Utah (Fig. 1) and is the third largest natural lake west of the Mississippi River in the USA, having a surface area of ~380 km² (Strong, 1974). Utah Lake is shallow with a mean depth of 2.8 m (Brimhall & Merritt, 1981) and is surrounded by an urban corridor and population has grown exponentially. For example, populations have grown from 60,000 to >630,000 within the last 50–60 years (Fig. 2; US Census Bureau, 2019; Williams, 2021). Utah Lake receives water from seven wastewater treatment plants (WWTP) in Utah Valley (Merritt & Miller, 2016) as well as storm-water runoff. In the past, the lake was also influenced by industrial plants, including a major steel (Geneva) mill, the Columbia Ironton pig iron plant (Larson, 1963), and the Tintic Standard Reduction Mill among others (Table 1).

In the last 30 years, HABs in Utah Lake may have increased in frequency, and in 2019, the Utah County Health Department installed its first permanent warning signs around the lake (Spangler, 2019). However, Tate (2019) concluded that water quality and HABs, on average, have not increased between 1984 and 2018 based on remote-sensing data. Whether or not HABs have increased or remained static over the last few decades, they remain a threat to the lake's ecosystem, including endemic endangered species such as *Chasmistes liorus*, or the June sucker.

A few modern studies indicate the state of nutrient loading and sources of AID in Utah Lake. Horns (2005) measured nutrient levels at inflows into the lake, including discharges from wastewater treatment plants (WWTPs) and stormwater. PSOMAS (2007) also documented eutrophication in the lake, including additional documentation of nutrient loads from anthropogenic sources where ~20% of P is from tributary streams that do not receive treated wastewater. Approximately 75% of P loading in Utah Lake was from wastewater, with the remainder from groundwater and miscellaneous surface sources. Spatially, the highest levels of sedimentary phosphorous are concentrated along the urban corridor on the east side of Utah Lake near WWTP inflows (Randall et al., 2019).

Utah Lake water quality affects wildlife and human populations, including downstream water users, as Utah Lake and Jordan River water is diverted for irrigation (UDWR, 2010). Utah Lake has been designated as a class 2A and 2B waterbody that classifies

Fig. 1 Index map showing Utah Lake and its surrounding regions, including core locations (red circles), streams, metal processing plants (green stars), and wastewater treatment plants (yellow circles) discussed in the text. Contours are elevations of the lakebed in meters
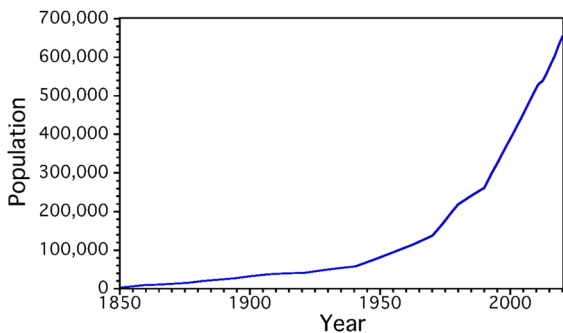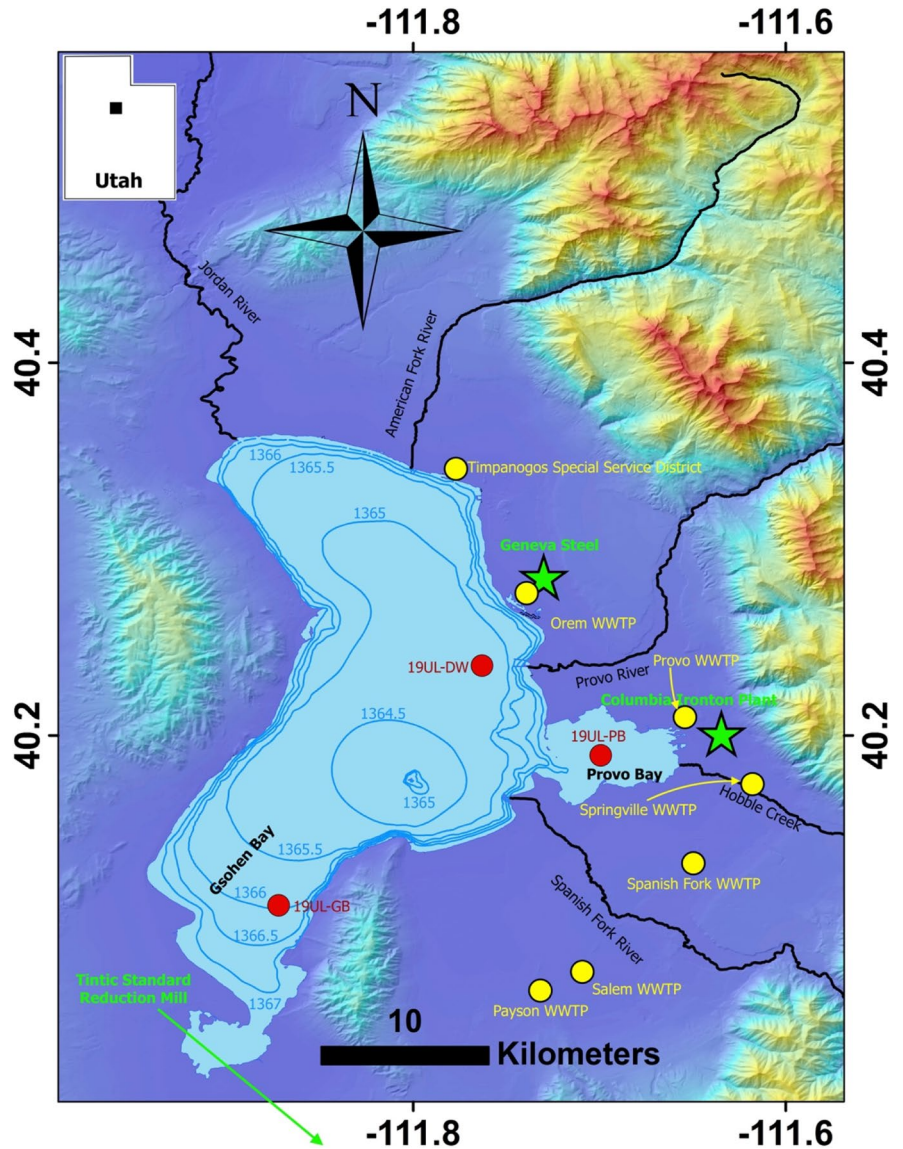

Fig. 2 Population growth in Utah County surrounding Utah Lake. See text for discussion

Utah Lake as an important recreational resource that should be safe for frequent primary contact, including potential ingestion, as well as being safe for infrequent primary contact, such as boating (DEQ, 2021). Utah Lake is also important for its esthetics given its proximity to a large population.

Globally, cyanotoxins have been responsible for many poisonings, some fatal and constant; low-concentration exposures have been linked to carcinogenic effects (Zanchett & Oliveria-Filho, 2013). Cyanotoxins from HABs are harmful to fish and are known to bioaccumulate in organisms, including fish (Zamora-Barrios et al., 2019), posing a problem for

Table 1 Historical events that may have impacted water quality in Utah Lake

Year	Description of event/activity
2002	Geneva Steel ceases operations
1970s	TEL stops being added to gasoline
1962	Columbia Ironton (pig iron and coke) Plant closes
1958	Orem Wastewater Treatment Plant is completed and begins operations
1950-1955	Provo Wastewater Treatment Plant is completed and begins operations
1944	Construction finished on Geneva Steel
1924	Construction completed for the Columbia Ironton (pig iron and coke) Plant
1924	Tintic Standard Reduction Mill closed
1920-1923	Construction and operation of the Tintic Standard Reduction Mill
1920s	TEL begins to be widely used as antiknock agent in gasoline
1882	Introduction of the common carp
1870-1880	Introduction of invasive *Phragmities australis* into Utah's waterways
1870	Mining begins in the Tintic Mountains
1849	Onset of European settlement of the Provo area

recreational angling in Utah Lake, where fish may be ingested by humans.

Irrigation diversions from Utah Lake and the Jordan River may also be problematic. Although the full range of the effects of cyanotoxins on agriculture is unknown, Xiang et al. (2019) demonstrated that microcystin, a dangerous cyanotoxin, can be taken up by crops via irrigation.

1.2 Geological Setting

Utah Lake occupies an intermontane valley formed by extension associated with the Great Basin over the last 17.5 Ma (e.g., Dickinson, 2006). The surrounding mountains are underlain by rocks ranging from Paleoproterozoic to Triassic in age (Constenius et al., 2011). Nearby to the east lies the Wasatch fault, at the eastern boundary of the Basin and Range Province (Machette et al., 1991). Major stream inflows cross the fault and include the Spanish Fork, American Fork, and Provo Rivers, as well as Hobble Creek. The only surface outflow is the Jordan River (Fig. 1), which connects Utah Lake to the Great Salt Lake. The other major water sink is evaporation, although ~7% of the water has been estimated to exit the basin through groundwater seepage (Horns, 2005; PSOMAS, 2007).

Utah Lake is a remnant of the larger Lake Bonneville system, which occupied Utah Valley between 21.9 and ~14.5 ka, based upon the elevation of preserved shorelines (Atwood et al., 2016) and the Lake

Bonneville hydrograph (Oviatt, 2015). Since the regression of Lake Bonneville, Utah Lake has preserved its own lacustrine sedimentary record. The pre-Bonneville sedimentary record is uncertain, but likely includes intercalated fluvial and lacustrine cycles in response to tectonic and climate variations. Recent sediment in Utah Lake is comprised mostly of endogenic calcite and detrital quartz, though minor dolomite and clays are present in some horizons (Randall et al., 2019).

2 Methods

2.1 Core Collection

Three freeze cores were collected from Utah Lake bottom sediments (Fig. 1; Table 2). Freeze coring limits disruption of the laminations of watery sediment and minimizes sediment deformation and compaction. All cores were obtained in August, 2019.

Table 2 UTM coordinates for freeze core collection sites

Core ID	UTM coordinates (UTM NAD83. Zone 12T)
19UL-DW (deep water near buoy)	435095E, 4454408N
19UL-GB (Goshen Bay)	425667E, 4440198N
19UL-PB (Provo Bay)	440472E, 4449007N

After coring, samples were stored and transported in dry ice. They were subsequently vacuum sealed in plastic sleeves and stored at −20 °C until processing.

Core 19UL-DW was collected near a buoy operated by the Utah Division of Water Quality and had a length of 76 cm. In addition to being co-located with the buoy, "DW" indicates that the core was located in relatively deep water (~3.5 m). Core 19UL-GB (GB=Goshen Bay) had a length of 55 cm and was collected in water ~1.5 m deep. Core 19UL-PB (PB=Provo Bay) had a length of 48 cm in water <1 m deep. Collectively, these three cores represent (a) a deep, open water setting close to densely populated areas (19UL-DW) and near the inflow of the Provo River; (b) an intermediate-depth, open-water setting removed from large populations (19UL-GB); and (c) a restricted bay with abundant emergent vegetation, shallow water, and heavy AID impacts (Fig. 1). This strategy gave the best opportunity to observe temporal changes in the lake across different environments.

2.2 Subsample Preparation

Cores were cut lengthwise into approximately $1 \times 1 \times 5$ cm cuboid subsamples and were measured using a digital caliper to estimate sediment volume. Since the outer surface of the frozen sediment may be irregular, deviations from true cuboid shapes were averaged. Sediment from the exterior of frozen subsamples was removed by scraping with a glass slide to reduce cross contamination. The mass of each frozen subsample was recorded, freeze-dried, and then reweighed. As such, all measurements were made on a dried-weight basis.

2.3 Sediment Ages

Samples were analyzed at the Science Museum of Minnesota using methods similar to Gunnell (2020). Ages were calculated based on ^{210}Pb activity measurements on an alpha spectrometer (Eakins & Morrison, 1978) using the constant rate of supply (CRS) model (Appleby, 2002) augmented by ^{137}Cs analysis via gamma spectrometry (Ritchie & McHenry, 1973) as an independent dating marker, designating the onset of atmospheric atomic bomb testing and its subsequent moratorium (ca. 1963). Lead-214 activity was also measured via gamma spectrometry as a secondary estimate of supported (background)

^{210}Pb activity in the sediments. The CRS model was chosen due to the potential for changes in sedimentation rates, as well as some sediment resuspension and mixing likely to occur in a shallow lake. Bulk wet and dry densities were used to calculate porosity.

2.4 X-Ray Diffraction

Quantitative mineralogical analyses were conducted using powder X-ray diffraction (XRD) at Brigham Young University (BYU) with a Rigaku Miniflex 600 equipped with a scintillation detector and graphite monochrometer. Freeze-dried, disaggregated samples were placed in the center cavity of zero background holders. Samples were analyzed from 3 to 65° 2θ. XRD and abundances were quantified via the Rigaku PDXL 2 software, using a Rietveld structure refinement method (e.g., Bish & Post, 1993).

The sediments were chiefly comprised of calcite, quartz, and dolomite. Small quantities of clay and other minerals were present in some samples. However, these were not included in the quantitative analysis. Due to overlapping peaks in complex mixtures, inclusion of phases that are not present can lead to false totals. Rather, we concentrated on tracking changes in endogenic versus detrital sedimentation (calcite:quartz ratios). Qualitatively, the presence of clay minerals was noted.

2.5 Nitrogen and Carbon Stable Isotopes

Values of $\delta^{15}N_{ATM}$ and $\delta^{12}C_{VPDB}$ of organic matter in the sediment samples were measured at the Stable Isotope Ratio Facility for Environmental Research (SIRFER) lab at the University of Utah. To remove carbonates, 300 mg of powdered subsamples was treated in 10% HCl and rinsed 4–5 times with deionized (DI) water. Samples were then freeze-dried for 48 h. Samples were analyzed at the SIRFER Lab by an isotope-ratio mass spectrometer coupled to an elemental analyzer. The isotopic analysis also quantified total nitrogen (TN) as well as total organic carbon (TOC) to a precision of 0.1 wt. %. Inorganic nitrogen (N_{inorg}) was estimated by the intercept method of Sampei and Matsumoto (2001) and subtracted.

2.6 Elemental Analysis

Concentrations of trace metals and total sedimentary phosphorous (TP) were measured by inductively coupled plasma-optical emission spectrometry (ICP-OES) at BYU. Materials were prepared similar to Yang et al. (2007) to release adsorbed as well as calcite-bound TP and trace metals. A total of 400±1 mg of sediment was refluxed in 16 ml of concentrated trace-metal grade HNO_3 acid for 1 h in Teflon beakers on a hotplate at ~100 °C. Samples were then centrifuged and the supernatant fluid was recovered for analysis. Samples were diluted 1:10 with deionized water and were analyzed in a ThermoFisher iCAP 7400 Duo ICP-OES instrument. Control solutions with a known concentrations were also analyzed every nine samples to continually check for instrumental drift. A solution of 16 ml of trace metal grade HNO_3 acid (sediment free) was similarly refluxed for every nine samples as blanks.

2.7 Pollen

Extraction from every other subsample from core 19UL-DW was performed in accordance with the University of Utah's Records of Environment and Disturbance (RED) Lab methodologies (Faegri & Iversen, 1989; Petersen et al., 1983). *Lycopodium* pollen was added to samples to act as an exotic tracer. Samples were digested with 10% HCl, then heated to 50 °C using a hot water bath in 10% KOH, and then further digested with concentrated HF. Samples were then treated with acetic anhydride and concentrated sulfuric acid for 2.0 to 2.5 min. Samples were placed in silicon oil and left to desiccate for 12 h. Slides were mounted using silicon oil and analyzed with a binocular microscope at 400× magnification. At least 200 non-tracer pollen grains were counted in each sample.

3 Results

3.1 Core Chronologies

^{210}Pb and ^{137}Cs chronologies were constructed for cores 19UL-GB and 19UL-PB (Table 3; Fig. 3). Both cores had low unsupported ^{210}Pb, but when augmented with ^{137}Cs counts, relatively good chronologies were established, especially for Provo Bay. Samples >35 cm depth in 19UL-GB were estimated to be pre-1950s based on ^{137}Cs results. Samples >40

Table 3 ^{210}Pb and ^{137}Cs activities for Utah Lake Cores

Core ID	Depth (cm)	^{210}Pb (total) (pCi/g)	^{214}Pb (pCi/g)	^{137}Cs (pCi/g)
19UL-GB	5–6	1.75	0.52	0.28
19UL-GB	11–12	1.18	0.81	0.22
19UL-GB	17–18	1.13	0.76	0.40
19UL-GB	23–24	1.02	0.69	0.28
19UL-GB	29–30	0.59	0.50	0.06
19UL-GB	37–38	**	**	Trace
19UL-PB	5–6	1.04	0.28	0.25
19UL-PB	11–12	1.04	0.62	0.37
19UL-PB	17–18	1.00	0.79	0.27
19UL-PB	23–24	1.12	0.53	0.24
19UL-PB	29–30	0.67	0.22	0.25
19UL-PB	35–36	**	**	0.18
19UL-PB	43–44	**	**	0.00
19UL-DW	1–2	**	**	Trace
19UL-DW	5–6	1.09	0.68	0.00
19UL-DW	11–12	1.20	0.71	0.00
19UL-DW	17–18	2.10	1.32	0.00
19UL-DW	23–24	0.53	1.01	0.00
19UL-DW	29–30	0.79	0.78	0.00

cm in 19UL-PB were also estimated to have been deposited pre-1950s.

19UL-DW did not have enough unsupported ^{210}Pb or measurable ^{137}Cs activities to establish a firm chronology. As a result, the relative pollen abundances from 19UL-DW pollen counts were used to help formulate an initial chronology. Pollen counts from 19UL-DW exhibited a drop in the relative percentage of Juniper pollen at 29 cm depth (Fig. 4). This decrease most likely represents land clearance for farming by European settlers, suggesting that all samples above 29 cm represent post-European colonization (post-1850s). In addition, multiple correlations to geochemical excursions between 19UL-DW with 19UL-GB and 19UL-PB provided additional confidence. For example, 19UL-GB and 19UL-PB both show increases in concentration in ^{15}N, Pb, Cu, and Zn between 1935 and 1940. These increases in concentrations were correlated to similar changes at 10 cm depth in 19UL-DW. Sediment above 10 cm was interpreted as being deposited post-1940s. Further extrapolation of the chronology of 19UL-DW prior to 1850 was made on the assumption of a constant rate of sedimentation.
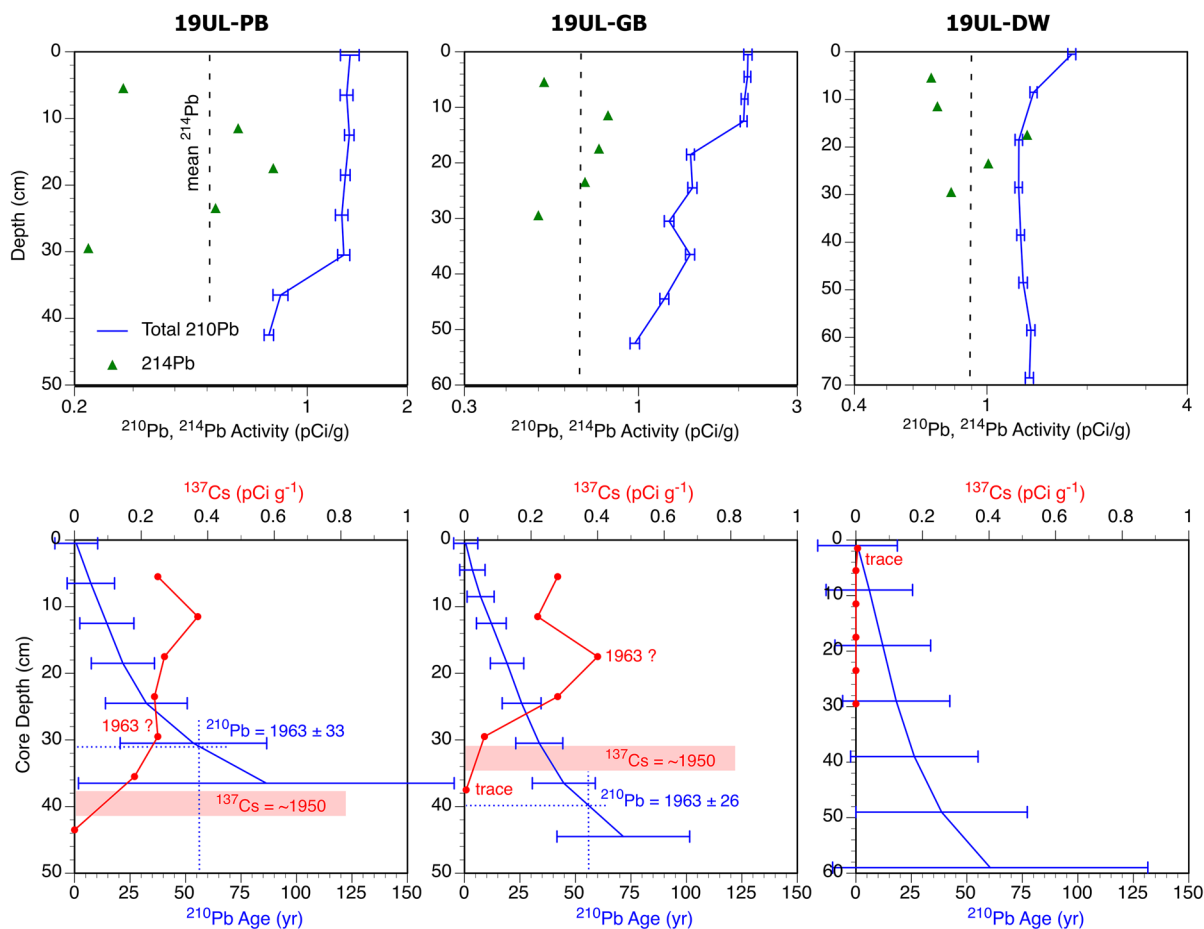
Fig. 3 Top row: depth versus activity relations for Utah Lake cores for ^{210}Pb and ^{214}Pb isotopes. Bottom row: age versus depth models, including ^{137}Cs results. Note that the deep-water core (19UL-DW) exhibited low unsupported activities and no detectable ^{137}Cs. See text for discussion

Overall, the ^{137}Cs and ^{210}Pb results contain significant uncertainty. However, two important conclusions can be confidently drawn: (a) the sediment in 19UL-DW deeper than ~30 cm was deposited well before European settlement and (b) the sediment in the other cores post-date pioneer settlement in ~1850.

3.2 Pollen

As noted above, pollen counts on 19UL-DW (Fig. 4) show that there was a discernable drop in the relative percentage of *Juniperus osteosperma* (Utah juniper) and CYPERACEAE (sedges) pollen at 29 cm. AMARANTHACEAE (beets, sugar beets, and others?) and POACEAE (native grasses and domesticated cereals?) relative percentages

both increased at 30 cm. *Quercus gambelii* (Gambel Oak), *Artemisia tridentate* (sagebrush), and PINACEAE (pine) pollen counts remained relatively constant throughout the core. *Typha latifolia* (cattail), SALICACEAE (willow), MALVACEAE, (mallow) BETULACEAE (birch), LILACAEAE (lilly), *Ephedra* (Mormon tea?), *Sambucus* (elderberry?), and *Sarcobatus* (greasewood & saltbrush) pollen were also present, although counts were low and relatively constant.

3.3 Mineralogy

The sediment of Utah Lake is a marl, consisting mostly of calcite, quartz, and dolomite, with minor amounts of smectite, muscovite/illite, and feldspars. As noted in the

Fig. 4 Pollen results from Williams (2021). Note that there is a distinct break in plant assemblages at ~1810 according to the ^{210}Pb chronology. This age was reset to 1850, coincident with European settlement and accompanying changes in the local flora of Utah Valley. See text for discussion
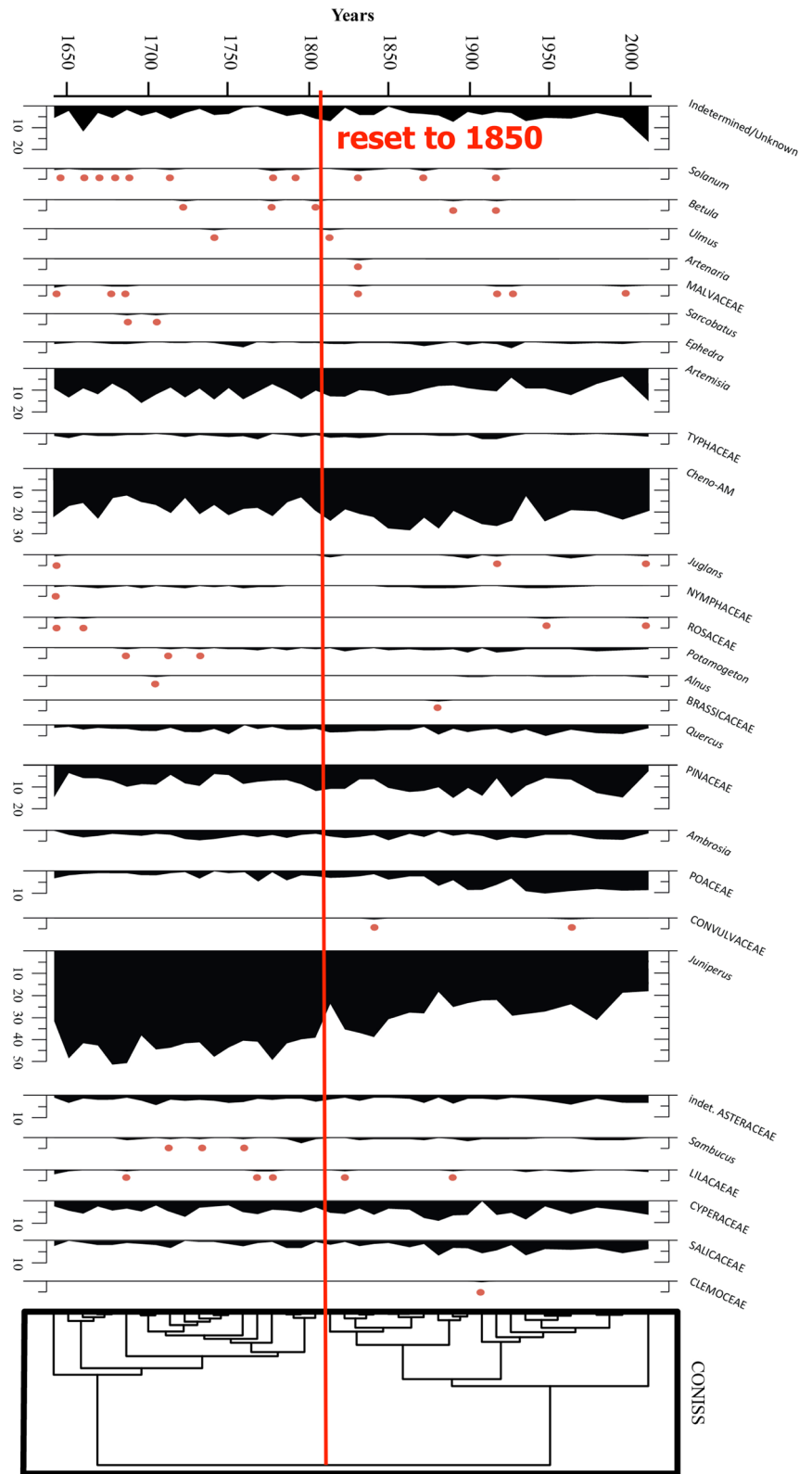
in the "Methods" section, aluminosilicate phases were excluded from quantification. Calcite is presumed to be primarily endogenic, whereas quartz and dolomite are detrital. The proportions of minerals with depth were generally constant, with calcite dominating 19UL-DW, 19UL-GB, and 19UL-PB at 80.9 ± 4.7, 78.8 ± 3.5, and $66.4\pm7.8\%$, respectively. Similarly, calcite:quartz ratios varied from 6.0 ± 0.7, 4.9 ± 0.6, to $2.6\pm1.2\%$. However, within an interval from 2000 to 2005, the calcite:quartz ratio increased dramatically from ~2 to ~6 in Provo Bay. In each core, there are intervals of clay present (Fig. 5), as indicated by broad (001) reflections at low 2θ (4–5°).

3.4 Nitrogen and Carbon Stable Isotopes and Abundances

This subsection presents the results of the analysis of organic C and N in the cores. However, in order to eliminate the overwhelming interference of inorganic carbon, these samples were leached in weak acid to eliminate carbonate as discussed in the "Methods" section. As a result, total organic carbon is reported as TOC_{acid}, where the material combusted via elemental analyzer was essentially organic matter and quartz.

3.4.1 Core 19UL-DW

At the base of this deep-water core, $\delta^{15}N$ values were relatively stable at ~6‰. However, beginning ~1940, $\delta^{15}N_{ATM}$ values increased to 8.6‰. N_{inorg} was estimated to be 0.14 wt. % of the total nitrogen. TN varied from 0.2 to 0.4 wt. % and was constant from the base upward until about 1930, after which it rose to 0.4 wt. % (Fig. 6). By contrast, $\delta^{13}C_{VPDB}$ values were relatively stable at ~−26.5‰, but became more negative beginning ~1940, reaching values of nearly −28.0‰ at the top of the core. Total organic carbon (TOC_{acid}) varied from 1.6 to 3.2 wt. %, with highest concentrations near the top of the core (Fig. 6). As might be expected, TOC_{acid} and TN strongly covary ($R^2=0.86$) as organic matter increased upward in the core. The ratio of C:N did not vary widely (mean=8.4) but decreased steadily after 1900 (Fig. 7).

Fig. 5 Calcite to quartz ratios for 19UL-DW (black), 19UL-GB (blue), and 19UL-PB (green) curves. The presence or absence of smectite or interlayered clays is also indicated and appear to be concurrent in the upper portions of 19UL-GB (blue) and 19UL-PB (green)
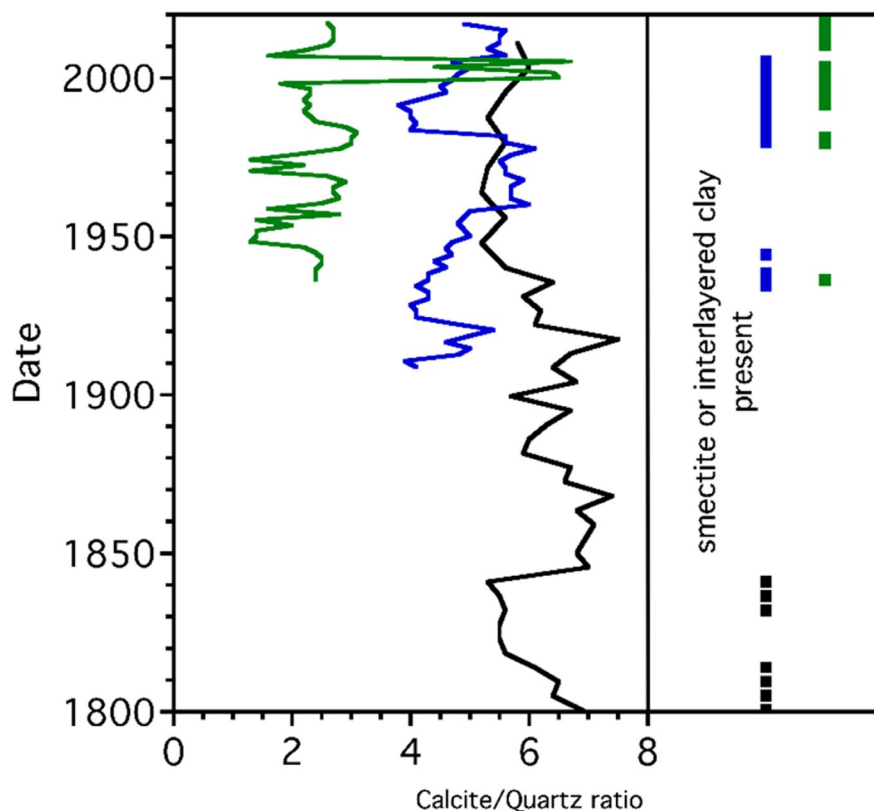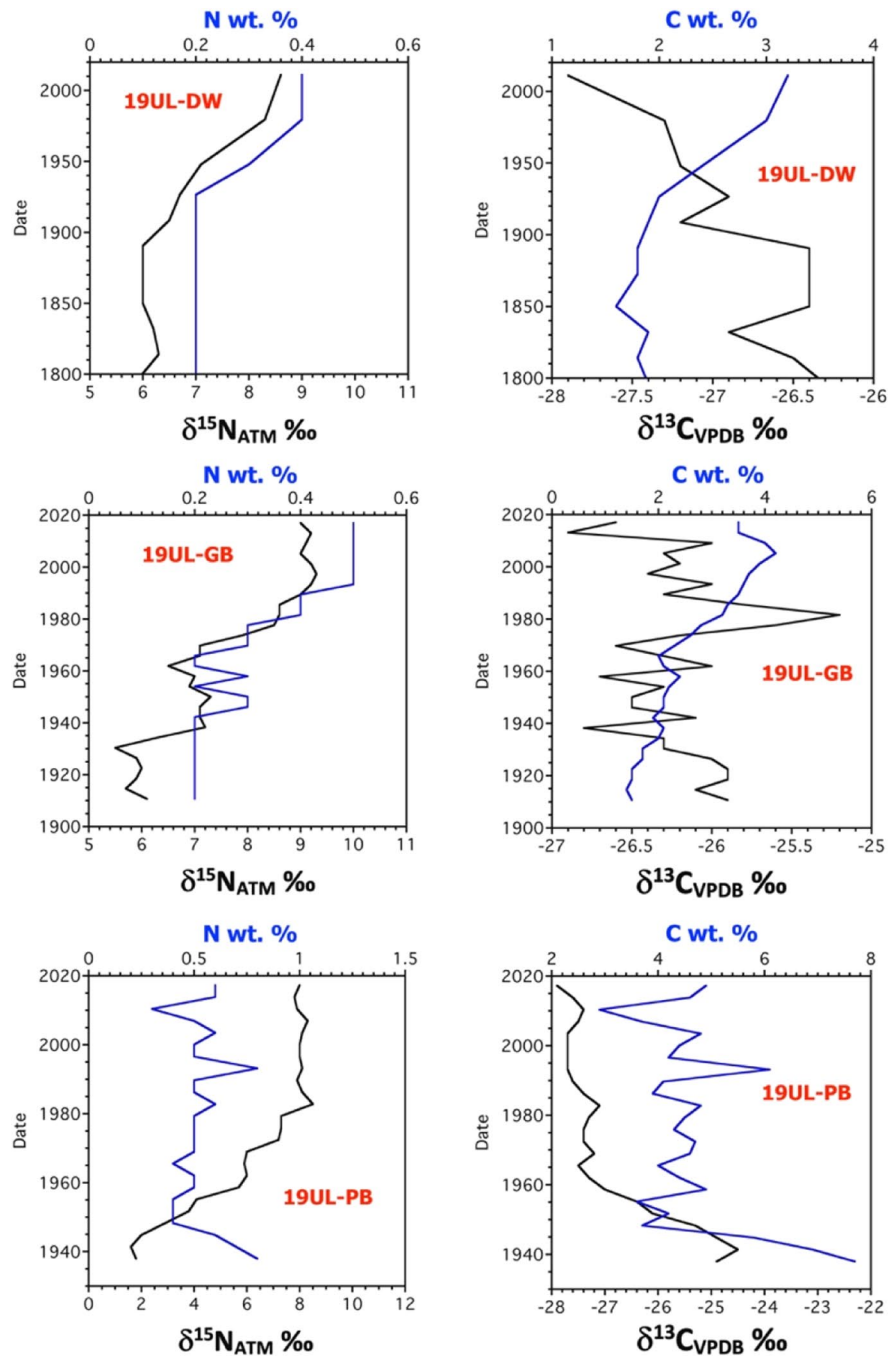
Fig. 6 Combined carbon—nitrogen ratio and abundance plots for Utah Lake cores

3.4.2 Core 19UL-GB

The Goshen Bay core also showed an enrichment in $\delta^{15}N_{ATM}$ values from ~6‰ after 1930–1940 to ~9‰. N_{inorg} was estimated to be 0.14 wt. % of the total nitrogen in this core as well. Isotopic enrichment appears to

have occurred in two steps. After 1940, values stabilized at ~7‰ until 1970 when values increased to towards the top of the core, stabilizing at about ~9‰ from 1990 to the present. The pattern of TN appears to match this trend, increasing from 0.2 to 0.5 wt.% near the top of the core (Fig. 6). $\delta^{13}C_{VPDB}$ values of 19UL-GB ranged from

−25.2 to −26.9‰ and show a slight negative, if variable trend. This pattern was matched by TOC_{acid} abundances, unlike 19UL-DW. In this core, organic matter abundances were highest at the base of the core, and TN and TOC_{acid} were highly correlated (R^2=0.98). C:N ratios decreased upward in the core from 9.5 to 7.1 in a well correlated manner (Fig. 7; R^2=0.60).

3.4.3 Core 19UL-PB

$\delta^{15}N_{ATM}$ values in ranged from <2.0 to 8.0–8.5‰, with a relatively steady TN content of ~0.5 wt. % (Fig. 6). N_{inorg} was estimated to be 0.10 wt. %. This core also showed an excursion toward larger $\delta^{15}N$ values beginning in ~1940 and stabilizing in the upper portion of the core beginning in ~1980. 19UL-3 $\delta^{13}C$ values ranged from −24.9 to −27.9‰ and became more depleted after 1940. Core 19UL-PB showed a strong negative excursion in $\delta^{13}C$ ratios from −24.5 to nearly −28‰. Since 1950, the $\delta^{13}C$ values in 19UL-PB and 19UL-DW have largely overlapped. Similar to TN, TOC_{acid} was fairly steady at ~4.0 wt. % (Fig. 6). TN and TOC_{acid} are highly correlated (R^2=0.84), and the C:N ratio is negatively correlated (R^2=0.76) with values ranging from 10 at the base to 8 at the top of the core (Fig. 7).
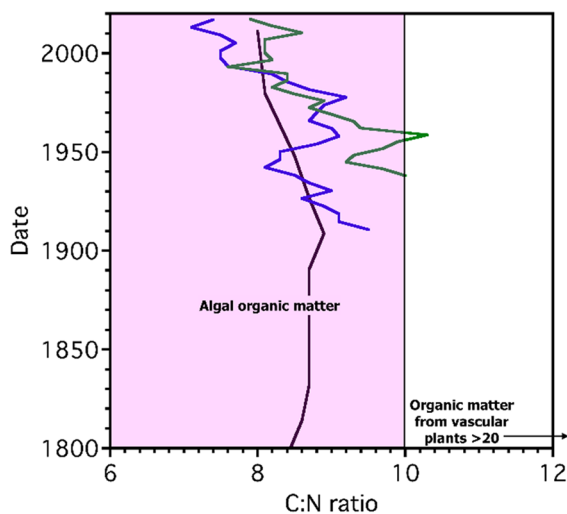
3.5 Total Phosphorous Concentrations

Total phosphorous (TP) concentrations showed systematic increases upward in each core (Fig. 8). TP concentrations in the bottom of core 19UL-DW were stable at ~800 mg/kg. After 1900, TP concentrations rose and reached 912 mg/kg at the top of the core with a maximum concentration of 1044 mg/kg in the 1990's. However, the increase in TP in this core was muted relative to the others.

TP concentrations in 19UL-GB began to increase in ~1940 and stabilized for nearly a decade at ~800–900 mg/kg (Fig. 8). TP then dropped for several years in the late 1950's and early 1960's to values similar pre-~1940. This was followed by a period of volatility between the mid 1960's and mid 1980's, after which TP concentrations increased to >1000 mg/kg.

At its base, TP concentrations in 19UL-PB are similar to those in the other cores, but they dramatically increased after 1940. At the base of the core, TP was ~800 mg/kg. Between 1940 and 1960, TP rose to ~1700 mg/kg or higher, with a maximum concentration of 1850 mg/kg reached in 1985. Between 1960 and the present, TP concentrations have remained relatively stable.
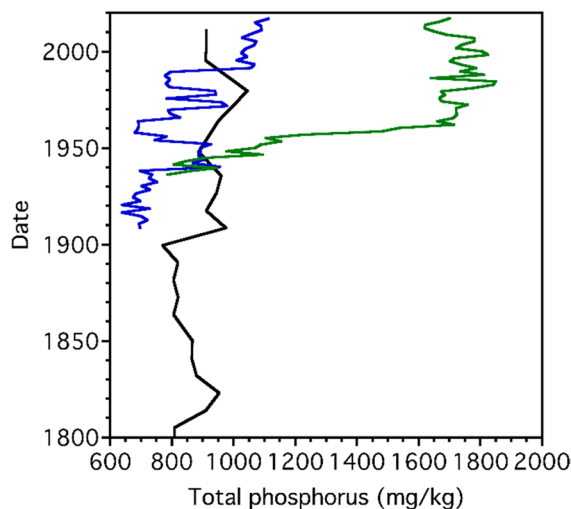

Fig. 7 Changes in the carbon to nitrogen ratio in Utah Lake cores as a function of time for 19UL-DW (black), 19UL-GB (blue), and 19UL-PB (green). All three cores exhibit ratios generally <10 and decreased throughout the twentieth and into the twenty-first centuries. These ratios suggest that the OM budget was dominated by algae and that algae have increased over time

Fig. 8 Total phosphorus versus time plot for 19UL-DW (black), 19UL-GB (blue), and 19UL-PB (green). Deep water sediment appears to be less affected by P loading than Goshen or Provo Bays

3.6 Trace Metals

Although this study focuses primarily on indicators of eutrophication, trace metal concentrations were measured simultaneously with TP. These ratios provide important information regarding AID in general, permit correlation between cores, and reveal average oxia/anoxia conditions in the lake. Regarding correlations, trace element patterns in these cores assisted in interpreting time-depth relations in 19UL-DW, which exhibited disappointing ^{210}Pb results. They also permit an assessment of the degree of resuspension and mixing of the sedimentary pile over time.

3.6.1 Trace Metal Stratigraphy

Lead (Pb) concentrations through time are illustrated in Fig. 9. Other metals such as Zn and Cu show very similar trends and were discussed further in Williams (2021). For example, the correlations (R^2) between Pb and Cu were 0.93, 0.89, and 0.85 for 19UL-DW, 19UL-GB, and 19UL-PB, respectively. Discussion will be centered on Pb as a representative trace metal and contaminant of concern within sediment.

From the base of the core to ~1880, Pb concentrations in 19UL-DW were constant at ~9–11 mg/kg. Beginning around 1880, Pb began to rise steadily until ~1940, after which it has remained high at variable concentrations centered around ~40 mg/kg for an overall four-fold increase (Fig. 9).

At ~1910, Pb concentrations in Goshen Bay were low at ~5 mg/kg. Beginning in ~1920, Pb concentrations rose steadily, reaching ~25 mg/kg in just a decade, where it stabilized until ~1965 when it increased again to ~30–35 mg/kg by ~1970 and has remained fairly stable since (Fig. 9).

Core 19UL-PB also exhibited a rise in Pb, beginning at ~4–5 mg/kg in 1940. Afterward, Pb rose steadily until ~1960 where it reached maximum concentrations of nearly 50 mg/kg. Between ~1960 and ~1980, Pb concentrations dropped to a value of ~35 mg/kg that has remained fairly constant (Fig. 9).

3.6.2 Oxia/Anoxia

The redox sensitive trace metals, vanadium (V) and nickel (Ni), are useful for establishing past average oxic, dysoxic, or anoxic conditions in the lake when they are normalized to Cr and Co, respectively. All samples from all three cores, regardless of age, plot in the oxic region of Fig. 10.
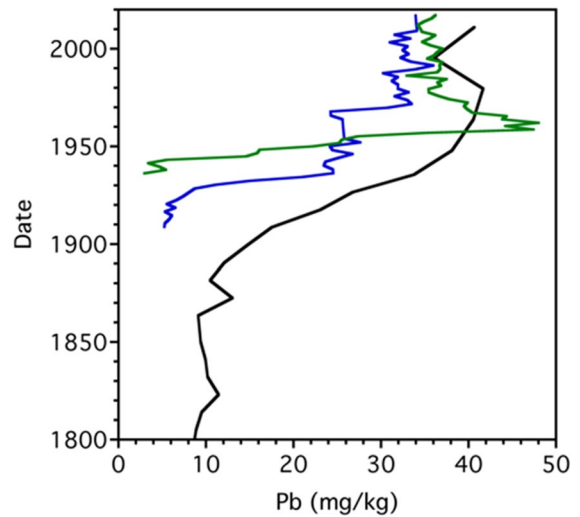

Fig. 9 Sedimentary Pb concentrations as a function of time for 19UL-DW (deep-water, black), 19UL-GB (Goshen Bay, blue), and 19UL-PB (Provo Bay, green). It appears that the entire lake was affected by anthropogenic heavy-metal loading

4 Discussion

Insights into the environmental stressors related to increasing populations around Utah Lake may be best obtained by examining the consequences of past development. To facilitate this retrospective analysis, we first evaluate the core chronologies, followed by consideration of pre-European lake conditions and the human-driven changes the lake has experienced. Finally, we suggest some benchmarks values for geochemical parameters in lake sediment that may be used to monitor ecosystem health and remedial progress.

4.1 Core Chronologies and Mixing

As reviewed above, the ^{210}Pb and ^{137}Cs core chronologies for 19UL-GB and 19UL-PB were employed to translate core depth to calendar date. However, due to the low activity of unsupported ^{210}Pb and ^{137}Cs that was below detection limit, the chronology of core 19UL-DW was quite uncertain. We have established a chronology for 19UL-DW based upon pollen analysis and correlation among other geochemical indices.

One process that may have erased the ^{210}Pb record is the pervasive resuspension of sediment during storm events. We consider this unlikely for

Fig. 10 Trace metal ratios indicating average redox conditions in Utah Lake sediments for 19UL-DW (black), 19UL-GB (blue), and 19UL-PB (green). Field values after Jones and Manning (1994)
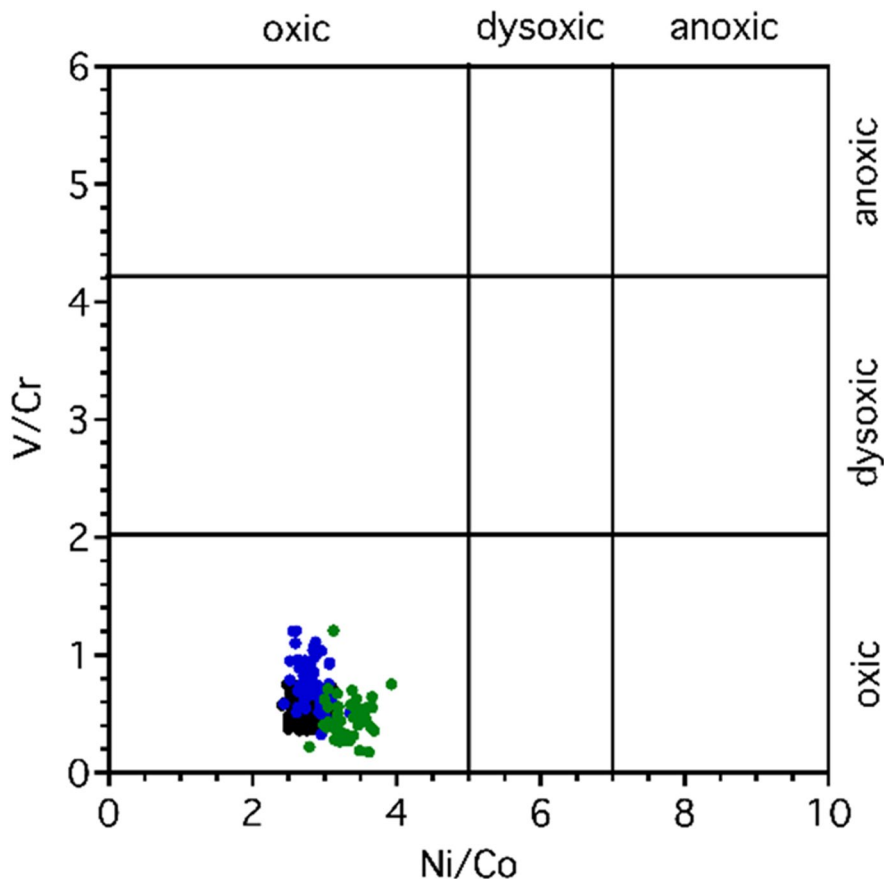
the following reasons. First, 19UL-DW was sampled in one of the deepest areas of the lake (Fig. 1) and it seems least likely that this core would be affected by resuspension and mixing (e.g., Dusini et al., 2009). Second, if these processes had homogenized the ^{210}Pb record, it should have homogenized other parameters as well. However, pollen, d^{15}N, d^{13}C, TP, and Pb values all show distinct temporal excursions in the core. This is especially true of Pb, which shows a 4-fold increase beginning ~1930. Although we cannot explain the ^{210}Pb and ^{137}Cs results beyond speculation that diffusive processes have altered the record, we are confident that 19UL-DW sediment has not been pervasively mixed.

4.1.1 19UL-DW Chronology

Based on the imprecise ^{210}Pb record from this core, the pollen assemblage shows a distinct break at an extrapolated date ~1810. We reset this horizon to 1850, or the timing of pioneer settlement in Utah Valley. After this time, juniper pollen decreases, likely in response to clearing of lands for farming and fuel. Simultaneously, the increases in grasses likely reflect the planting of cereal crops and the increase in chenopods may represent the increase in weeds or crops like sugar beets, which were introduced to Utah in the early 1850s (UHE, 2021).

The pollen record leads to a chronology based on these points: 1850 at 29 cm, 1940 at 10 cm, and 2019 at the top of the core. Before 1850, ages are inferred by extrapolation. This is, of course, a very imprecise chronology, yet it still suggests that the major changes seen in geochemical proxies occurred post-1940s, which is in general agreement with the other cores. 19UL-DW also records a much lower sedimentation rate (~0.15 cm/yr) than 19UL-GB (~0.51 cm/yr) and 19UL-PB (~0.57 cm/yr). Despite the imprecision, the low sedimentation rate and depth of the 19UL-DW ensure that a lengthy episode of pre-European settlement conditions were recorded.

4.2 Nutrients Across Pre- to Post-European Settlement

Of the three cores, only 19UL-DW extends back in time pre-European time. Thus, this core is discussed first and is employed to infer conditions within the lake prior to pioneer settlement. Subsequently, all three cores are discussed to examine subsequent changing lake conditions. In fact, a comparison of 19UL-DW to the other cores suggests that many of the proxies remained in near-pristine conditions until the mid-twentieth century.

4.2.1 19UL-DW Geochemical Indicators

C:N ratios suggest that algae were the dominant source of OM in the cores (Fig. 7). The OM from vascular plants typically has a C:N ratio of >20, whereas algae vary between 4 and 10. This ratio is usually preserved in subaqueous environments (Jasper & Gagosian, 1990; Meyers, 1994). A value of ~8.0 is also consistent with the C:N ratio of organic matter in sediment traps (Prahl et al., 1980) that is dominated by planktic sources (Ishiwatari and Uzaki, 1987).

4.2.2 Cross-Core Synthesis

Our preferred interpretation from the deep-water core is that the pre-European OM budget was dominated by algae and that planktic and benthic primary producers have remained the dominant and increasing source of OM in Utah Lake sediment as evidenced by the low and decreasing C:N ratios in all three cores since the mid-twentieth century (Fig. 7).

As discussed in the "Results" section, calcite:quartz ratios, except for some excursions, are relatively uniform in all three cores (Fig. 5). In nearby Farming Bay, and over the same time frame, Gunnell et al. (2022) observed increasing endogenic carbonate production rates that were driven by increased algal productivity, where removal of dissolved CO_2 during photosynthesis elevated lake pH. In Utah Lake, increased algal productivity is reflected only in the C:N ratios. In summary, it appears that endogenic calcite production rates (Fig. 5) as well as algal productivity (Fig. 7) have been elevated throughout Utah Lake's history. It seems likely that the water column has always been turbid due to algae and endogenic calcite nucleation and

that future remediation efforts are unlikely to produce a clear water column. However, reduction of nutrient fluxes may clearly mitigate the frequency and intensity of HABs.

Although nitrogen isotopes do not directly infer N-loading, they are very useful in evaluating nitrogen sources. Until ~1950, $d^{15}N$ was stable at 6.0–6.5‰, consistent with natural nitrogen sources. The excursion to higher $d^{15}N$ after ~1950 implies increasing contributions of ^{15}N-enriched AID sources such as wastewater discharge and runoff impacted by animal waste (Clark & Fritz, 1997; Fig. 5) that are associated with population growth (Fig. 2).

Beyond population growth and associated increases in AIDs, a holistic view of C and N abundances strongly implies that there has been significant increase in N-loading to the lake. Although TOC_{acid} and TN abundances were fairly constant in Provo Bay, both increased with time in 19UL-DW and 19UL-GB (Fig. 6), reflecting increased productivity and burial of OM. However, these increases accompanied decreases in C:N ratios (Fig. 7). These relationships require that the relative proportion of N increased at a greater rate than the overall burial of OM.

Carbon-isotope trends are more difficult to interpret. $\delta^{13}C$ values from all three cores range from −27.9 to −24.5‰ (Fig. 6), well within C3 plant ranges (−22 to −29‰; Clark & Fritz, 1997). Although the decline in $\delta^{13}C$ with time is difficult to explain in detail, the excursions may be due to major changes in the lake's ecology. A possible contribution to declining $\delta^{13}C$ may be the expansion of *Phragmites australis,* which has a measured $\delta^{13}C$ between −27 and −28‰ (Choi et al., 2005; Gichuki et al., 2001). However, C:N ratios infer that the sedimentary OM budget is controlled by algae. We suggest that changes have occurred in algal communities toward ^{13}C-depleted taxa, as signatures in $\delta^{13}C$ and C:N ratios appear to be preserved during burial diagenesis (e.g., Meyers, 1994). However, this must be viewed with caution. Higher productivity is often associated with enrichment, rather than depletion, in the ^{13}C content of OM (e.g., Lücke et al., 2003), although high pH conditions during blue-green algal blooms may produce ^{13}C depletion (Herczeg & Fairbanks, 1987).

Sediment of the deep-water core exhibited only modest increases in TP (Fig. 8), suggesting that open and deep portions of the lake are not sequestering

large quantities of phosphorus from AID. Rather, elevated TP is concentrated near sites of wastewater inputs (e.g., Randall et al., 2019) or in other isolated or semi-isolated areas like Goshen and Provo Bays. Nonetheless, the rise of P concentrations above background values in all three cores, starting in the early 1900s, is probably best explained by increased nutrient loading from AID (Jarvie et al., 2006). The very high P concentrations in Provo Bay may be due to the wastewater treatment plants, which discharges effluent into Provo Bay, and does not mix efficiently with the rest of the lake (Bradshaw et al., 1976).

The stabilization of P levels after 1960 in Provo Bay may be due to the sediment reaching its maximum P adsorption capacity (Zhang et al., 2016) or due to improved P removal by improved treatment practices. The earlier shift to higher concentrations of P after 1880 in 19UL-DW, which is near the Provo River outflow, was likely due to the growth of Provo City, which was founded next to the Provo River in 1849 (Moffitt, 1975). In summary, nutrient loadings have affected the lake unevenly, as reflected in surface sediments (Randall et al., 2019), but also through time as indicated here.

4.3 Trace Metals Across Pre- to Post-European Settlement

The increase in trace metals mimic the rise in TP to a large degree, although they came primarily from industrial sources, urban runoff (e.g., Davis et al., 2001), and the deposition of coal combustion aerosols (e.g., Hower et al., 2008; Kong et al., 2011; Czech et al., 2020), rather than agricultural sources and treated wastewater. The rise of Pb (and Cu, Zn) concentrations started as early as 1920 (Fig. 9) well before the construction of Geneva Steel, but at about the same time that tetra-ethyl lead was introduced into gasoline (Seyferth, 2003; Siver & Wozniak, 2001) and the Ironton pig-iron plant was constructed and producing coke (Whetten, 2011). This plant operated from the 1920s until it closed in 1962 (EPA, 2000; Moffitt, 1975) (Table 1).

The Geneva plant produced steel using coal-derived coke (Whetten, 2011), and as such would have been a major source of heavy metals during operation. In addition, coal has been a major source

of electrical generation and was widely used for home heating until the 1950s (USU, 2022). The Tintic Standard Refinement Mill south of Goshen Bay (Fig. 1; James, 1984) may also have contributed metals to the lake, although its operational lifespan was short (SAH, 2021; Table 1).

In summary, abundant heavy-metal sources have been present in and around Utah Lake for more than a century, and much of can be clearly linked to heavy industry (e.g., Romano et al., 2018; Smith et al., 2009). Major mining and steel production has discontinued around Utah Lake, with the last being Geneva Steel, which closed in 2002 (Table 1). However, over the last several decades since the 1960s to 1970s, Pb concentrations have reached a steady state or even declined somewhat in Provo Bay (Fig. 9). It appears that the decommissioning of industrial facilities has been approximately offset by increased urban sources such as road runoff (Carling et al., 2015; Legret & Pagotto, 1999; Rice et al., 2002), heavy metals in treated sewage effluent (Wang et al., 2005), and other urban sources (Gnecco et al., 2005).

4.4 Long-Term Lake Redox

Much like Pb, redox sensitive V and Ni concentrations show increasing trends towards the top of the cores, albeit the signals are noisier and muted compared to Pb (Fig. 21 in Williams, 2021). Increasing V and Ni concentrations were most likely derived from fossil fuel combustion (Hope, 1997) and other metal production facilities (Poznanović Spahić et al., 2019) and not lake anoxia (Huang et al., 2015). Co and Cr concentrations also showed increasing concentrations post-1950s which may have been due to increased steel production from Geneva Steel and the Columbia Ironton Plants (Fig. 22 in Williams, 2021).

The redox state of sediment suggests that Utah Lake is well oxygenated on average (Riquier et al., 2006) (Fig. 10), which is expected in a shallow lake that is regularly mixed by wave action (Shaw et al., 2004). The overall oxic state of the lake indicates that anoxia driven by algal blooms is temporary. Excursions into anoxic conditions are either too short to be recorded or are erased near the sediment-water interface when oxic conditions return. The overall oxic state of Utah Lake, however, does not mean that algal blooms are benign events.

5 Summary and Conclusions

The cores collected and analyzed in this study permit the evaluation of changes in Utah Lake from before 1850, the onset of European Settlement, to the present. Establishing age-depth relationships in these alkaline lake cores was challenging. Good ^{210}Pb and ^{137}Cs age chronologies were obtained for two of the cores and extended to the third via correlation. Overall, changes in core proxies correlated well with the timing of anthropogenic drivers summarized in Table 1.

Pollen assemblages in the deep water core indicate profound changes on the surrounding landscape occurred at this time due to the clearing of native vegetation and planting food crops. Total phosphorus, carbon, and nitrogen isotope and abundance data indicate that (a) the C:N ratios of the OM budget of the lake have been dominated by algal contributions, (b) that those algal contributions are, if anything, increasing, (c) that d^{13}C values indicate that there has been a major reorganization of algal communities, and (d) that nutrient loading has variably affected the lake. TP in the deep-water core has increased only modestly, whereas in Goshen and especially Provo Bay, it has increased dramatically. In fact, in Provo Bay, TP has more than doubled since ~1940 and remained fairly stable since ~1960 (Fig. 8).

Trace metals have also greatly impacted lake sediment, and unlike TP, the impacts are apparent in all cores. Trace metals have a greater ability to impact the entire lake suggesting that they are not as rapidly bound and transferred as TP into the sediment or that atmospheric dispersal and deposition have played a larger role. Although the lake has always been turbid due to endogenic calcite production and algae in the water column, AID has had a major impact to lake ecology.

Most importantly, this study can be used to establish easily measured benchmarks for future sediment sampling to monitor ecosystem health and remediation impacts by comparison to pre-European values summarized in Table 4. Although it may be unrealistic to expect a return to pre-European conditions, intermediate goals between pre-settlement and modern values could be set. The parameters are summarized in Table 4. The placement and monitoring of sediment traps may be the most effective method of monitoring the health of the lake and, hopefully, its recovery.

Data Availability   All data are publicly available, either in Tables, or in the MS Thesis of Richard Williams (Williams, 2021) available at https://scholarsarchive.byu.edu/etd/.

Declarations

Conflict of Interest   The authors declare no competing interests.

Table 4 Comparison of easily measured proxies of ecosystem health and nutrient loading. Pre-European values establish baseline values for assessing improvements in ecosystem health

Parameter	Pre-European value	Current value
d^{15}N	2 to 6‰	8–10‰
d^{13}C	−25 to −26.5‰	−27 to −28‰
TN	0.2% in open water	0.4 to 0.5 % in open water
C:N	8.5 to 10	7.5 to 8
TP	700 to 800 mg/kg	1000 to 1800 mg/kg
Pb	4 to 10 mg/kg	25 to 48 mg/kg

References

Appleby, P. G. (2002). Chronostratigraphic techniques in recent sediments. In W. M. Last & J. P. Smol (Eds.), *Tracking Environmental Change Using Lake Sediments* (Vol. 1). Springer.

Atwood, G., Wambeam, T. J., & Anderson, N. J. (2016). The present as a key to the past: Paleoshoreline correlation insights from Great Salt Lake. In *Developments in Earth Surface Processes* (Vol. 20, pp. 1–27).

Bish, D. L., & Post, J. E. (1993). Quantitative mineralogical analysis using the Rietveld full-pattern fitting method. *American Mineralogist, 78*(9-10), 932–940.

Bradshaw, J. S., Sundrud, R. B., Barton, J. R., Fuhriman, D. K., Loveridge, E. L., & Pratt, D. R. (1976). Chemical response of Utah Lake to nutrient inflow. *Water Pollution Control Federation, 45*, 880–887.

Brimhall, W. H., & Merritt, L. B. (1981). Geology of Utah Lake: Implications for resource management. *Great Basin Naturalist Memoirs, 5*, 24–42.

Burford, M. A., Carey, C. C., Hamilton, D. P., Huisman, J., Paerl, H. W., Wood, S. A., & Wulff, A. (2020). Perspective:

Advancing the research agenda for improving understanding of cyanobacteria in a future of global change. *Harmful Algae, 9.* https://doi.org/10.1016/j.hal.2019.04.004

Carling, G. T., Tingey, D. G., Fernandez, D. P., Nelson, S. T., Aanderud, Z. T., Goodsell, T. H., & Chapman, T. R. (2015). Evaluating natural and anthropogenic trace element inputs along an alpine to urban gradient in the Provo River, Utah, USA. *Applied Geochemistry, 63,* 398–412. https://doi.org/10.1016/j.apgeochem.2015.10.005

Census Bureau, U. S. (2019). *QuickFacts Utah; Utah County, Utah.* United States Census Bureau https://www.census.gov/quickfacts/fact/table/utahcountyutah/PST045219#PST045219

Chislock, M. F., Doster, E., Zitomer, R. A., & Wilson, A. E. (2013). Eutrophication: Causes, consequences, and controls in aquatic ecosystems. *Nature Education Knowledge, 4,* 10.

Choi, W., Ro, H., & Chang, S. X. (2005). Carbon isotope composition of *Phragmites australis* in a constructed saline wetland. *Aquatic Botany, 82,* 27–38. https://doi.org/10.1016/j.aquabot.2005.02.005

Clark, I. D., & Fritz, P. (1997). *Environmental isotopes in hydrogeology.* Lewis.

Constenius, K. N., Clark, D. L., King, J. K., & Ehler, J. B. (2011). *Interim geologic map of the Provo 30' X 60' Quadrangle, Utah, Wasatch and Salt Lake Counties, Utah.* Open-File Report. Utah Geological Survey.

Czech, T., Marchewicz, A., Sobczyk, A. T., Krupa, A., Jaworek, A., & Rosiak, D. (2020). Heavy metals partitioning in fly ashes between various stages of electrostatic precipitator after combustion of different types of coal. *Process Safety and Environmental Protection, 133,* 18–31.

Davis, A. P., Shokouhian, M., & Ni, S. (2001). Loading estimates of lead, copper, cadmium, and zinc in urban runoff from specific sources. *Chemosphere, 44,* 997–1009.

DEQ (Utah Department of Environmental Quality). (2021). Accessed November 12, 2021, from https://documents.deq.utah.gov/water-quality/standards-technical-services/DWQ-2021-017555.pdf.

Dickinson, W. R. (2006). Geotectonic evolution of the Great Basin. *Geosphere, 2*(7), 353–368. https://doi.org/10.1130/GES00054.1

Dusini, D. S., Foster, D. L., Shore, J. A., & Merry, C. (2009). The effect of Lake Erie water level variations on sediment resuspension. *Journal of Great Lakes Research, 35*(1), 1–12. https://doi.org/10.1016/j.jglr.2008.04.001

Eakins, J. D., & Morrison, R. T. (1978). A new procedure for the determination of lead-210 in lake and marine sediments. *The International Journal of Applied Radiation and Isotopes, 29,* 531–536.

EPA. (2000). *Provo City Steeling Itself for Redevelopment* (Vol. 5150, p. 2). US Environmental Protection Agency Outreach and Special Projects Report.

Faegri, K., & Iversen, J. (1989). *Textbook of pollen analysis* (4th ed.). John Wiley & Sons.

Gichuki, J., Treist, L., & Dehairs, F. (2001). The use of stable carbon isotopes as tracers of ecosystem in functioning wetland ecosystems of Lake Victoria, Kenya. *Hydrobiologia, 458,* 91–97. https://doi.org/10.1023/A:1013188229590

Gnecco, I., Berretta, C., Lanza, L. G., & La Barbera, P. (2005). Storm water pollution in the urban environment of Genoa, Italy. *Atmospheric Research, 77*(1-4), 60–73. https://doi.org/10.1016/j.atmosres.2004.10.017

Gunnell, N., Nelson, S. T., Rushforth, S., Rey, K., Hudson, S. M., Carling, G., Miller, T., Meyers, L., & Engstrom, D. (2022). From hypersaline to fresh-brackish: Documenting the impacts of human intervention on a natural water body from cores, Farmington Bay, UT, USA. *Water, Air, and Soil Pollution, 233.* https://doi.org/10.1007/s11270-022-05507-x

Gunnell, N. V. (2020). *A study of the anthropogenic impact in Farmington Bay through isotopic and elemental analysis* (p. 77). Brigham Young University MS Thesis.

Herczeg, A. L., & Fairbanks, R. G. (1987). Anomalous carbon isotope fractionation between atmospheric CO2 and dissolved inorganic carbon induced by intense photosynthesis. *Geochimica et Cosmochimica Acta, 51,* 895–899.

Hope, B. K. (1997). An assessment of the global impact of anthropogenic vanadium. *Biogeochemistry, 37,* 1–13.

Horns, D. (2005). Utah Lake comprehensive management plan: Resource document. In *Fires and State Land.* Department of Forestry.

Hower, J. C., Graham, U. M., Dozier, A., Tseng, M. T., & Khatri, R. A. (2008). Association of the sites of heavy metals with nanoscale carbon in a Kentucky electrostatic precipitator fly ash. *Environmental Science & Technology, 42*(22), 8471–8477.

Huang, J., Huang, F., Evans, L., & Glasauer, S. (2015). Vanadium: Global (bio)geochemistry. *Chemical Geology, 417,* 68–89. https://doi.org/10.1016/j.chemgeo.2015.09.019

Ishiwatari, R., & Uzaki, M. (1987). Diagenetic changes of lignin compounds in a more than 0.6 million-year-old lacustrine sediment (Lake Biwa, Japan). *Geochimica et Cosmochimica Acta, 51*(2), 321–328.

James L.P., 1984. The Tintic mining district. *Survey Notes.* 18(2). Utah Geological and Mineral Survey.

Jarvie, H. P., Neal, C., & Withers, P. (2006). Sewage-effluent phosphorus: A greater risk to river eutrophication than agricultural phosphorus? *Science of The Total Environment, 360,* 246–253. https://doi.org/10.1016/j.scitotenv.2005.08.038

Jasper, J. P., & Gagosian, R. B. (1990). The sources and deposition of organic matter in the Late Quaternary Pigmy Basin, Gulf of Mexico. *Geochimica et Cosmochimica Acta, 54,* 1117–1132.

Jones, B., & Manning, D. A. (1994). Comparison of geochemical indices used for the interpretation of palaeoredox conditions in ancient mudstones. *Chemical Geology, 111,* 111–129.

Kong, S., Lu, B., Ji, Y., Zhao, X., Chen, L., Li, Z., Han, B., & Bai, Z. (2011). Levels, risk assessment and sources of PM10 fraction heavy metals in four types dust from a coal-based city. *Microchemical Journal, 98*(2), 280–290.

Landsberg, J. H. (2002). The effects of harmful algal blooms on aquatic organisms. *Reviews in Fisheries Science, 10,* 113–390. https://doi.org/10.1080/20026491051695

Larson, G. O. (1963). Bulwark of the kingdom: Utah's iron and steel industry. *Utah Historical Quarterly, 31,* 248–261.

Legret, M., & Pagotto, C. (1999). Evaluation of pollutant loadings in the runoff waters from a major rural highway. *The*

Science of the Total Environment, 235, 143–150. https://doi.org/10.1016/S0048-9697(99)00207-7

Lücke, A., Schleser, G. H., Zolitschka, B., & Negendank, J. F. (2003). A Lateglacial and Holocene organic carbon isotope record of lacustrine palaeoproductivity and climatic change derived from varved lake sediments of Lake Holzmaar, Germany. *Quaternary Science Reviews, 22*, 569–580.

Machette, M. N., Personius, S. F., Nelson, A. R., Schwartz, D. P., & Lund, W. R. (1991). The Wasatch Fault Zone, Utah, segmentation and history of Holocene earthquakes. *Journal of Structural Geology, 13*, 137–149. https://doi.org/10.1016/0191-8141(91)900062-N

Merritt, L. B., & Miller, W. A. (2016). Nutrient loading to Utah Lake. In *Utah Lake Studies*. Farmington Bay and Utah Lake Water Quality Council.

Meyers, P. A. (1994). Preservation of elemental and isotopic source identification of sedimentary organic matter. *Chemical Geology, 114*, 289–302.

Moffitt, J. C. (1975). *The story of Provo*. Press Publishing Company.

Oviatt, C. G. (2015). Chronology of Lake Bonneville, 30,000 to 10,000 yr BP. *Quaternary Science Reviews, 110*, 166–171.

Petersen, K. L., Mehringer, P. J., Jr., & Gustafson, C. E. (1983). Late-glacial vegetation and climate at the Manis Mastodon Site, Olympic Peninsula, Washington. *Quaternary Research, 20*, 215–231.

Poznanović Spahić, M. M., Sakan, S. M., Glavaš-Trbić, B. M., Tančić, P. I., Škrivanj, S. B., Kovačević, J. R., & Manojlović, D. D. (2019). Natural and anthropogenic sources of chromium, nickel and cobalt in soils impacted by agricultural and industrial activity (Vojvodina, Serbia). *Journal of Environmental Science and Health Part A, 54*, 219–230. https://doi.org/10.1080/10934529.2018.1544802

Prahl, F. G., Bennett, J. T., & Carpenter, R. (1980). The early diagenesis of aliphatic hydrocarbons and organic matter in sedimentary particulates from Dabob Bay, Washington. *Geochimica et Cosmochimica Acta, 44*, 1967–1976.

PSOMAS. (2007). *Utah Lake TMDL: Pollutant loading assessment and designated beneficial use impairment assessment*. Prepared for: State of Utah Division of Water Quality.

Randall, M. C., Carling, G. T., Dastrup, D. B., Miller, T., Nelson, S. T., Rey, K. A., Bickmore, B. R., & Aanderud, Z. T. (2019). Sediment potentially controls in-lake phosphorous cycling and harmful cyanobacteria in shallow eutrophic Utah Lake. *PLoS One*. https://doi.org/10.1371/journal.pone.0212238

Rice, K. C., Conko, K. M., & Hornberger, G. M. (2002). Anthropogenic sources of arsenic and copper to sediments in a Suburban Lake, North Virginia. *Environmental Science and Technology, 36*, 4962–4967. https://doi.org/10.1021/es025727x

Riquier, L., Tribovillard, N., Averbuch, O., Devleeschouwer, X., & Riboulleau, A. (2006). The Late Frasnian Kellwasser horizons of the Harz Mountains (Germany): Two oxygen-deficient periods resulting from different mechanisms. *Chemical Geology, 233*, 137–155. https://doi.org/10.1016/jchemgeo.2006.02.021

Ritchie, J. C., & McHenry, J. R. (1973). Determination of fallout 137Cs and naturally occurring gamma-ray emitters in sediments. *The International Journal Of Applied Radiation And Isotopes, 24*, 575–578. https://doi.org/10.1016/0020-708X(73)90125-7

Romano, E., Bergamin, L., Magno, M. C., Pierfranceschi, G., & Ausili, A. (2018). Temporal changes of metal and trace element contamination in marine sediments due to a steel plant: The case study of Bagnoli (Naples, Italy). *Applied Geochemistry, 88*(A). https://doi.org/10.1016/j.apgeochem.2017.05.012

SAH (Society of Architectural Historians), 2021. Accessed November 11, 2021, from https://sah-archipedia.org/buildings/UT-01-049-0063.

Sampei, Y., & Matsumoto, E. (2001). C/N ratios in a sediment core from Nakaumi Lagoon, southwest Japan—Usefulness as an organic source indicator. *Geochemical Journal, 35*, 189–205.

Seyferth, D. (2003). The rise and fall of tetraethyllead. 2. *Organometallics*, *22*(25). https://doi.org/10.1021/om030621b. American Chemical Society.

Shaw, B. H., Mechenich, C., & Klessig, L. L. (2004). *Understanding Lake Data*. Board of Regents of the University of Wisconsin System.

Siver, P. A., & Wozniak, J. A. (2001). Lead analysis of sediment cores from seven Connecticut lakes. *Journal of Paleolimnology, 26*, 1–10. https://doi.org/10.1023/A:1011131201092

Smith, J. N., Lee, K., Gobeil, C., & Macdonald, R. W. (2009). Natural rates of sediment containment of PAH, PCB and metal inventories in Sydney Harbour, Nova Scotia. *Science of the Total Environment, 407*, 4858–4869. https://doi.org/10.1016/j.scitotenv.2009.05.029

Smith, V. H., & Schindler, D. W. (2009). Eutrophication science: Where do we go from here? *Trends in Ecology and Evolution, 24*, 201–207.

Spangler, D. K. (2019). *Algal blooms abound: Permanent signs tell about risks*. Utah Department of Environmental Quality. https://deq.utah.gov/communication/news/algal-blooms-abound-permanent-sings-tell-about-risks

Strong, A. E. (1974). Remote sensing of algal blooms by aircraft and satellite in Lake Erie and Utah Lake. *Remote Sensing of the Environment, 3*, 99–107. https://doi.org/10.1016/0034-4257(74)90052-2

Tate, R. S. (2019). *Landsat collections reveal long-term algal bloom hot spots of Utah Lake* (p. 47). Brigham Young University M.S. thesis.

UDWR (Utah Division of Water Resources) (2010). Jordan River Basin; Planning for the Future. Utah State Water Plan. www.water.utah.gov

UHE (Utah History Encyclopedia) 2021. Accessed December 8, 2021, from https://www.uen.org/utah_history_encyclopedia/s/SUGAR_INDUSTRY.shtml.

USU (Utah State University) 2022. Accessed March 18, 2022, from https://extension.usu.edu/rangelands/ou-files/RRU_Section_Eight_Energy.pdf

Wang, C., Hu, X., Chen, M., & Wu, Y. (2005). Total concentrations and fractions of Cd, Cr, Pb, Cu, Ni, and Zn in sewage sludge from municipal and industrial wastewater treatment plants. *Journal of Hazardous Material, 119*, 245–249. https://doi.org/10.1016/j.jhazmat.2004.11.023

Whetten, C. L. (2011) "This strange enterprise": Geneva steel and the American west (pp. 81). The University of Utah. MS thesis.

Williams, R. R. R. (2021). *Determining the anthropogenic effects on eutrophication of Utah Lake since European settlement using multiple geochemical approaches* (p. 47). Brigham Young University M.S. thesis.

WS (Web of Science) 2021. Accessed November 11, 2021, from https://www.webofscience.com/wos/woscc/basic-search.

Xiang, L., Li, Y., Liu, B., Zhao, H., Li, H., Cai, Q., Mo, C., Wong, M., & Li, Q. X. (2019). High ecological and human health risks from microcystins in vegetable fields in southern China. *Environmental International, 133*, 105–142. https://doi.org/10.1016/j.envint.2019.105142

Yang, H., Linge, K., & Rose, N. (2007). The Pb pollution fingerprint at Lochnagar: The historical record and current status of Pb isotopes. *Environmental Pollution, 145*, 723–729. https://doi.org/10.1016/j.envpol.2006.06.026

Zamora-Barrios, C. A., Nandini, S., & Sarma, S. S. S. (2019). Bioaccumulation of microcystins in seston, zooplankton and fish: A case study in Lake Zumpango, Mexico. *Environmental Pollution, 249*, 267–276. https://doi.org/10.1016/j.envpol.2019.03.029

Zanchett, G., & Oliveria-Filho, E. C. (2013). Cyanobacteria and cyanotoxins: From impacts on aquatic ecosystems and human health to anticarcinogenic effects. *Toxins, 5*, 1896–1917. https://doi.org/10.3390/toxins5101896

Zhang, L., Du, Y., Du, C., Xu, M., & Loaiciga, H. A. (2016). The adsorption/desorption of phosphorus in freshwater sediments from buffer zones: The effects of sediment concentration and pH. *Environmental Monitoring and Assessment, 188*. https://doi.org/10.1007/s10661-015-5018-0

Zhu, G., Wang, F., Zhang, Y., Gao, G., & Qin, B. (2008). Hypoxia and its environmental influences in large, shallow, and eutrophic Lake Taihu, China. *Internationale Vereinigung für Theoretische und Angewandte Limnologie: Verhandlungen, 30*, 361–365. https://doi.org/10.1080/03680770.2008.11902144